View Article Online / Journal Homepage / Table of Contents for this issue

Published on 27 April 2011. Downloaded by University of Chicago on 30/10/2014 19:42:54.

This article is published as part of the *Dalton Transactions* themed issue entitled:

d^0 organometallics in catalysis

Guest Editors John Arnold (UC Berkeley) and Peter Scott (University of Warwick)

Published in issue 30, 2011 of *Dalton Transactions*

Image reproduced with permission of Guo-Xin Jin

Articles in the issue include:

PERSPECTIVES:

Half-titanocenes for precise olefin polymerisation: effects of ligand substituents and some mechanistic aspects
Kotohiro Nomura and Jingyu Liu
Dalton Trans., 2011, DOI: 10.1039/C1DT10086F

ARTICLES:

Stoichiometric reactivity of dialkylamine boranes with alkaline earth silylamides
Michael S. Hill, Marina Hodgson, David J. Liptrot and Mary F. Mahon
Dalton Trans., 2011, DOI: 10.1039/C1DT10171D

Synthesis and reactivity of cationic niobium and tantalum methyl complexes supported by imido and β-diketiminato ligands
Neil C. Tomson, John Arnold and Robert G. Bergman
Dalton Trans., 2011, DOI: 10.1039/ C1DT10202H

Visit the *Dalton Transactions* website for more cutting-edge inorganic and organometallic research
www.rsc.org/dalton

Dalton Transactions

Dynamic Article Links

Cite this: *Dalton Trans.*, 2011, **40**, 7718

www.rsc.org/dalton

PAPER

Published on 27 April 2011. Downloaded by University of Chicago on 30/10/2014 19:42:54.

Synthesis and reactivity of cationic niobium and tantalum methyl complexes supported by imido and β-diketiminato ligands†

Neil C. Tomson, John Arnold* and Robert G. Bergman*

Received 6th February 2011, Accepted 4th April 2011
DOI: 10.1039/c1dt10202h

The synthesis and reactivity of the cationic niobium and tantalum monomethyl complexes [(BDI)MeM(N^{t}Bu)][X] (BDI = [Ar]NC(CH$_3$)CHC(CH$_3$)N[Ar], Ar = 2,6-^{i}Pr$_2$C$_6$H$_3$; M = Nb, Ta; X = MeB(C$_6$F$_5$)$_3$, B(C$_6$F$_5$)$_4$] was investigated. The cationic alkyl complexes failed to irreversibly bind CO but formed phosphine-trapped acyl complexes [(BDI)(R$_3$PC(O)Me)M(N^{t}Bu)][B(C$_6$F$_5$)$_4$] (R = Et, Cy) in the presence of a combination of trialkylphosphines and CO. Treatment of the monoalkyl cationic Nb complex with XylNC (Xyl = 2,6-Me$_2$-C$_6$H$_3$) resulted in irreversible formation of the iminoacyl complex [(BDI)(XylN═C(Me))Nb(N^{t}Bu)][B(C$_6$F$_5$)$_4$], which did not bind phosphines but would add a methide group to the iminoacyl carbon to provide the known ketimine complex (BDI)(XylNCMe$_2$)Nb(N^{t}Bu). Further stoichiometric chemistry explored i) migratory insertion reactions to form new alkoxide, amidinate, and ketimide complexes; ii) protonolysis reactions with Ph$_3$SiOH to form thermally robust cationic siloxide complexes; and iii) catalytic high-density polyethylene formation mediated by the cationic Nb methyl complex.

Introduction

Cationic complexes of the d^0 early-metal alkyls have shown increased reactivity compared to their neutral counterparts. This effect has been attributed variously to (i) the formation of lower-coordinate complexes, which have an increased number of metal-based orbitals available for binding and activating a substrate; (ii) a decrease in the formal electron count at the metal, which enhances the metal-based electrophilicity; and (iii) the polarization of the M–C bond.[1–7] Study of the metallocenium alkyl complexes has contributed greatly to the development of these principles, largely due to an interest in understanding their activity as olefin polymerization catalysts.[8–11]

Recent research in Ziegler-type olefin polymerization has focused on the development of ligand sets that may impart steric or electronic effects different from those observed for the metallocenes.[12–20] The imido ligand has been used in this context, leading to imido-supported early-metal alkyl cations with olefin polymerization activities rivalling those of the metallocenes.[3,21–23] Despite these advances in catalytic systems, the stoichiometric chemistry of these complexes has remained relatively unexplored.

One question of particular interest to the imido-supported cations is the behavior of the imido group. In contrast to the metallocene systems in which the Cp ligands are generally non-reactive, the imido functionality is well-known to effect a range of [2 + 2], C–H activation, and nucleophilic substitution reactions when bound to the more electropositive early-metals.[24–32] This reactivity creates a question of site-selectivity when early-metal imido compounds have alkyl groups bound to them, since early-metal alkyl groups may also react with unsaturated and protic reagents to form insertion and protonolysis products.

We[2] and others[33–37] have initiated studies aimed at understanding this reaction site selectivity, including how a cationic charge at such imido-supported alkyl complexes may affect the observed reactivity. The present work details our investigations into the synthesis and reactivity of well-defined cationic alkyl complexes of the heavier Group 5 metals supported by the *tert*-butylimido (N^{t}Bu) ligand and the bulky, bidentate *N*,*N*′-diaryl-β-diketiminate (BDI, aryl = 2,6-^{i}Pr$_2$-C$_6$H$_3$) ligand set.

Experimental

General considerations

Unless otherwise noted, all reactions were performed using standard Schlenk line techniques or in an MBraun dry box under an atmosphere of nitrogen (<1 ppm O$_2$/H$_2$O). All glassware, cannulae, and Celite were stored in an oven at *ca.* 425 K. Pentane, Et$_2$O, and THF were purified by passage through a column of activated alumina and degassed prior to use.[38] C$_6$H$_5$F and C$_6$H$_5$Cl were distilled from CaH$_2$ and stored over activated 4 Å molecular sieves. Deuterated solvents were vacuum-transferred from sodium/benzophenone (benzene) or calcium hydride (chlorobenzene). NMR spectra were recorded on Bruker AV-300, AVQ-400

Department of Chemistry, University of California, Berkeley, California, USA 94720. E-mail: arnold@berkeley.edu, rbergman@berkeley.edu; Tel: +1–510–643–5181 (JA) and +1–510–642–2156 (RGB)

† Complete crystallographic data for compounds **2a**, **4**, and **5** is available. CCDC reference numbers 675085, 808678 and 808679. For crystallographic data in CIF format see DOI: 10.1039/c1dt10202h

This journal is © The Royal Society of Chemistry 2011

Published on 27 April 2011. Downloaded by University of Chicago on 30/10/2014 19:42:54.

and DRX-500 spectrometers. ^{1}H and $^{13}C\{^{1}H\}$ chemical shifts are given relative to residual solvent peaks; ^{19}F chemical shifts are referenced to external $CFCl_3$ at 0.0 ppm; and $^{31}P\{^{1}H\}$ chemical shifts are given relative to an external standard of $P(OMe)_3$ set to 1.67 ppm. Proton and carbon NMR assignments were routinely confirmed by ^{1}H–^{1}H (COSY) or ^{1}H–^{13}C (HMQC and HMBC) experiments. Infrared (IR) samples were prepared as Nujol mulls and were taken between KBr disks. The following chemicals were purified prior to use: $TaCl_5$ by sublimation; acetophenone was stored over 4 Å molecular sieves, which had been dried under vacuum for 12 h at 120 °C prior to use; $B(C_6F_5)_3$ was purified by sublimation. $Li(BDI)\cdot OEt_2$,[39] $py_2Cl_3Ta(N^tBu)$,[40] $[(Et_2O)_2H][B(C_6F_5)_4]$,[41] and $(BDI)Me_2Nb(N^tBu)$[42] (**1**) were prepared using the literature procedures. All other reagents were acquired from commercial sources and used as received. Elemental analyses were determined at the College of Chemistry, University of California, Berkeley. The X-ray structural determinations were performed at CHEXRAY, University of California, Berkeley.

Crystallographic analysis

Single crystals of **2a**, **4**, and **5** were coated in Paratone-N oil, mounted on a Kaptan loop, transferred to a Siemens SMART diffractometer or a Bruker APEX CCD area detector,[43] centered in the beam, and cooled by a nitrogen flow low-temperature apparatus that had been previously calibrated by a thermocouple placed at the same position as the crystal. Preliminary orientation matrices and cell constants were determined by collection of 60 10 s frames, followed by spot integration and least-squares refinement. An arbitrary hemisphere of data was collected, and the raw data were integrated using SAINT.[44] Cell dimensions reported were calculated from all reflections with $I > 10$ (Table 1). The data were corrected for Lorentz and polarization effects, but no correction for crystal decay was applied. Data were analyzed for agreement and possible absorption using XPREP.[45] An empirical absorption correction based on comparison of redundant and equivalent reflections was applied using SADABS.[46] Structures were solved by direct methods with the aid of successive difference Fourier maps and were refined against all data using the SHELXTL 5.0 software package. Thermal parameters for all non-hydrogen atoms were refined anisotropically, except in solvent molecules disordered over multiple partially occupied positions. ORTEP diagrams were created using the ORTEP-3 software package.[47]

[(BDI)MeNb(N^{t}Bu)][B(C$_6$F$_5$)$_4$] (2a) from [(Et$_2$O)$_2$H][B(C$_6$F$_5$)$_4$]

A solution of $[(Et_2O)_2H][B(C_6F_5)_4]$ (200 mg, 0.24 mmol) in Et_2O (6 mL) was added to a solution of **1** (148 mg, 0.24 mmol) in Et_2O (4 mL) at room temperature. The color immediately turned from pale yellow to bright yellow and the solution effervesced rapidly. After 10 min at room temperature, the solution was concentrated to *ca*. 3 mL and filtered to give a clear yellow solution. The filtrate was stored at −35 °C for 24 h during which time a crystalline material formed. The solid was collected by filtration and dried under vacuum. Yield: 251 mg, 81%. While **2a** proved to be more thermally robust than **1**, isolated samples of **2a** were stored in a −35 °C freezer to prevent decomposition. ^{1}H NMR (400 MHz, C_6D_5Cl): δ 7.25–7.05 (m, 6H, Ar), 5.86 (s, 1H, *H*C(C(Me)NAr)$_2$), 2.13 (sept, 2H, C*H*Me$_2$), 1.88 (s, 6H, HC(C(*Me*)NAr)$_2$), 1.82 (sept, 2H, C*H*Me$_2$), 1.21 (d, 6H, CH*Me*$_2$), 1.06 (d, 6H, CH*Me*$_2$), 1.00 (d, 6H, CH*Me*$_2$), 0.95 (s, 3H, Nb*Me*), 0.88 (d, 6H, CH*Me*$_2$), 0.71 (s, 9H, ^{t}Bu). $^{13}C\{^{1}H\}$ NMR (125.7 MHz, C_6H_5F/ 10% C_6D_6, 298 K): δ 171.6, 142.5, 140.4, 139.8, 129.3, 125.9, 124.9, 96.3, 76.5, 48.5, 32.8, 31.2, 29.2, 25.7, 24.9, 24.5, 24.2, 23.8. ^{19}F NMR

Table 1 Crystallographic data for compounds **2a, 4**, and **5**

Compound	**2a**·2Et$_2$O	**4**·0.5hexane	**5**
Formula	$C_{66}H_{73}BF_{20}N_3NbO_2$	$C_{41}H_{62}Cl_2N_4Ta$	$C_{34.86}H_{55.58}Cl_{0.14}N_3Ta$
Formula weight	1423.99	862.80	702.65
Space Group	$P\bar{1}$	$P\bar{1}$	$P2_1/c$
a (Å)	13.616(3)	10.4181(10)	10.4872(15)
b (Å)	16.444(3)	12.5964(12)	13.1367(19)
c (Å)	17.040(3)	16.7145(16)	24.997(4)
α (°)	114.348(2)	84.9620(10)	90
β (°)	102.282(3)	76.5520(10)	93.375(2)
γ (°)	91.108(3)	74.7490(10)	90
V (Å^3)	3371.6(11)	2057.4(3)	3437.8(9)
Z	2	2	4
ρ_{calcd} (g cm^{-3})	1.403	1.393	1.421
F_{000}	1464	886	1508
μ (cm^{-1})	0.28	0.28	0.33
T_{min}/T_{max}	0.815713	0.840323	0.75191
No. rflns measured	12 998	11 261	21 789
No. indep. rflns	7758	7455	8300
R_{int}	0.0334	0.0128	0.0491
No. obs. ($I > 2.00\sigma(I)$)	5193	6827	6457
No. variables	838	433	363
R_1, wR_2[a]	0.0513, 0.1153	0.0248, 0.0619	0.0371, 0.0739
R_1 (all data)	0.0935	0.0286	0.0540
GoF	1.054	1.267	0.991
Res. peak/hole (e$^-$/Å^3)	0.885/−0.437	2.594/−0.641	1.406/−0.615

[a] $R_1 = \sum(|F_o| - |F_c|)/\sum(|F_o|)$; $wR_2 = [\sum\{w(F_o^2 - F_c^2)^2\}/\sum\{w(F_o^2)^2\}]^{1/2}$.

Published on 27 April 2011. Downloaded by University of Chicago on 30/10/2014 19:42:54.

(376.5 MHz, C_6D_5Cl, 298 K): δ –130.70 (s, *o*-F, $B(C_6F_5)_4$), –161.43 (t, *m*-F, $B(C_6F_5)_4$), –165.24 (t, *p*-F, $B(C_6F_5)_4$). Anal. Calcd for $C_{58}H_{53}BF_{20}N_3Nb$: C, 54.60; H, 4.19; N, 3.29. Found: C, 54.53, H 4.08; N, 3.24.

[(BDI)MeNb(N^{t}Bu)][$B(C_6F_5)_4$] (2a) from [Ph_3C][$B(C_6F_5)_4$]

A solution of [Ph_3C][$B(C_6F_5)_4$] (15 mg, 0.016 mmol) in C_6D_5Cl (0.5 mL) was added to a solution of **1** (10 mg, 0.016 mmol) in C_6D_5Cl (0.5 mL). The color of the solution immediately turned bright yellow. The sample was analyzed spectroscopically, without purification; ^{1}H and ^{19}F NMR data indicated a mixture of **2a** and 1,1,1-triphenylethane.

[(BDI)MeNb(N^{t}Bu)][$MeB(C_6F_5)_3$] (2b)

A solution of $B(C_6F_5)_3$ (101 mg, 0.12 mmol) in Et_2O (5 mL) was added to a solution of **1** (75 mg, 0.12 mmol) in Et_2O (5 mL) at room temperature. The color of the solution immediately turned from pale yellow to bright yellow. Removal of the volatile materials under vacuum provided a yellow oil, from which a solid deposited on addition of pentane (10 mL). The solid was collected, washed again with pentane (2 × 10 mL), and dried under vacuum to give a pale yellow powder. Yield: 80 mg, 87%. ^{1}H NMR (400 MHz, C_6D_5Cl): δ 7.20 (m, 2H, Ar), 7.08 (m, 4H, Ar), 5.93 (s, 1H, *H*C(C(Me)NAr)$_2$), 2.20 (sept, 2H, ^{i}Pr-C*H*), 1.92 (s, 6H, HC(C(*Me*)NAr)$_2$), 1.88 (sept, 2H, ^{i}Pr-C*H*), 1.25 (d, 9H, ^{i}Pr-*Me* and *Me*B), 1.10 (d, 6H, ^{i}Pr-*Me*), 1.05 (d, 6H, ^{i}Pr-*Me*), 1.01 (s, 3H, Nb*Me*), 0.92 (d, 6H, ^{i}Pr-*Me*), 0.75 (s, 9H, ^{t}Bu). ^{19}F NMR (376.5 MHz, C_6D_5Cl): δ –130.70 (d, $MeB(C_6F_5)_3$, *o*-F), –163.20 (t, $MeB(C_6F_5)_3$, *m*-F), –165.64 (t, $MeB(C_6F_5)_3$, *p*-F). Anal. Calcd for $C_{53}H_{56}BF_{15}N_3Nb$: C, 56.65; H, 5.02; N, 3.74. Found: C, 56.55, H, 5.18; N, 4.05.

(BDI)pyCl_2Ta(N^{t}Bu) (4)

THF (20 mL) was added to a flask containing a solid mixture of py$_2Cl_3$Ta(N^{t}Bu) (500 mg, 0.97 mmol) and LiBDI·OEt_2 (483 mg, 0.97 mmol) at room temperature. The resulting solution was stirred and heated to 65 °C for 12 h; the color turned progressively orange throughout the course of the reaction. The volatile materials were removed under vacuum and the product was extracted with Et_2O (2 × 15 mL) and filtered to give a clear orange filtrate. The solution was concentrated to 10 mL and stored at –80 °C for 1 week. The orange crystals that precipitated from solution were collected by filtration and dried under vacuum. Yield: 360 mg, 45%. X-ray quality crystals were grown from a saturated hot hexane solution (+65/+25 °C). ^{1}H NMR (500 MHz, C_6D_6, 298 K): δ 8.60 (d, 2H, py), 7.19 (br s, 3H, Ar), 7.09 (br m, 1H, Ar), 7.02 (br m, 2H, Ar), 6.62 (br s, 1H, py), 6.26 (br s, 2H, py), 5.22 (s, 1H, *H*C(C(Me)NAr)$_2$), 3.86 (br s, 2H, C*H*Me$_2$), 3.70 (br s, 2H, C*H*Me$_2$), 1.80 (br s, 6H, CH*Me*$_2$), 1.78 (br s, 3H, HC(C(*Me*)NAr)$_2$), 1.63 (br s, 3H, HC(C(*Me*)NAr)$_2$), 1.28 (br s, 6H, CH*Me*$_2$), 1.04 (br s, 6H, CH*Me*$_2$), 0.99 (br s, 6H, CH*Me*$_2$), 0.68 (s, 9H, ^{t}Bu).

(BDI)Me_2Ta(N^{t}Bu) (5)

A solution of **4** (320 mg, 0.39 mmol) in Et_2O (25 mL) was cooled to 0 °C and stirred vigorously as MeMgBr (0.26 mL, 0.78 mmol, 3.0 M solution in Et_2O) was added dropwise by syringe. The color immediately turned pale yellow from bright orange as a white precipitate developed from the solution. The cold bath was removed and the slurry was stirred at room temperature for 10 min. Removal of the volatile materials under vacuum resulted in a pale yellow solid. The product was extracted with hexane (2 × 15 mL) and the resulting solution was filtered and concentrated to 10 mL. Storing the solution at –40 °C induced crystallization of the product within 12 h. The crystalline material was collected by filtration and dried under vacuum. Yield: 202 mg, 74%. ^{1}H NMR (500 MHz, C_6D_6, 293 K): δ 7.13 (br s, 6H, Ar), 5.22 (s, 1H, *H*C(C(Me)NAr)$_2$), 3.08 (br m, 4H, C*H*Me$_2$), 1.63 (s, 6H, HC(C(*Me*)NAr)$_2$), 1.37 (br d, 12H, CH*Me*$_2$), 1.14 (d, 12H, CH*Me*$_2$), 1.10 (s, 9H, ^{t}Bu), 0.59 (s, 6H, Nb*Me*$_2$). ^{13}C{^{1}H} NMR (125.7 MHz, C_6D_6, 298 K): δ 167.1, 141.9, 126.7, 124.7, 103.3, 64.6 (^{t}Bu, C$_\alpha$) 58.3 (Ta*Me*$_2$), 32.2 (^{t}Bu, C$_\beta$), 29.1, 26.8, 25.1, 25.0. Anal. Calcd for $C_{35}H_{56}N_3Ta$: C, 60.07; H, 8.07; N, 6.00. Found: C, 59.90, H, 8.21; N, 5.96.

[(BDI)MeTa(N^{t}Bu)][$B(C_6F_5)_4$] (6)

Solid [$(Et_2O)_2H$][$B(C_6F_5)_4$] (993 mg, 1.20 mmol) was added in portions to a solution of **5** (847 mg, 1.21 mmol) in fluorobenzene (10 mL). The solution rapidly effervesced as the color turned slightly more golden yellow. The solution was stirred for 10 min at room temperature, then the volatile materials were removed under vacuum. The resulting oil was washed with pentane (2 × 10 mL) and the remaining solvent was removed under vacuum to give a foam, which was crushed and washed thoroughly with pentane (2 × 10 mL). The residual solvent was again removed under vacuum, leaving a yellow solid, which was crushed into a fine pale green–yellow powder and collected. Yield: 1.50 g, 91%. ^{1}H NMR (300 MHz, C_6H_5Cl/ 10% C_6D_6): δ 5.81 (s, 1H, *H*C(C(Me)NAr)$_2$), 2.18 (sept, 2H, C*H*Me$_2$), 2.06 (sept, 2H, C*H*Me$_2$), 1.88 (s, 6H, HC(C(*Me*)NAr)$_2$), 1.25 (d, 6H, CH*Me*$_2$), 1.08 (d, 6H, CH*Me*$_2$), 1.02 (d, 6H, CH*Me*$_2$), 0.89 (d, 6H, CH*Me*$_2$), 0.81 (s, 3H, Ta*Me*), 0.70 (s, 9H, ^{t}Bu). ^{13}C{^{1}H} NMR (125.7 MHz, C_6H_5F/ 10% C_6D_6, 298 K): δ 173.5, 142.0, 141.0, 140.6, 130.6, 126.0, 125.0, 95.7, 71.7 (^{t}Bu, C$_\alpha$) 54.0 (Ta*Me*), 32.7, 32.5 (^{t}Bu, C$_\beta$), 29.3, 25.5, 25.1, 24.4, 24.0, 23.6. ^{19}F NMR (376.5 MHz, C_6H_5Cl/10% C_6D_6): δ –130.90 (s, *o*-F, $B(C_6F_5)_4$), –161.61 (t, *m*-F, $B(C_6F_5)_4$), –165.42 (t, *p*-F, $B(C_6F_5)_4$). Anal. Calcd for $C_{58}H_{53}BF_{20}N_3Ta$: C, 51.08; H, 3.92; N, 3.08. Found: C, 50.79, H 4.04; N, 3.18.

General procedure for the synthesis of [(BDI)(η^2-OC(Me)(PR_3))M(N^{t}Bu)] [$B(C_6F_5)_4$] (7a, 7b, 8a, 8b)

The methyl-bound cation (0.15 mmol) and phosphine (0.45 mmol) were dissolved in fluorobenzene (10 mL) and added to a 50 mL Schlenk flask. The flask was cooled to –40 °C, then the headspace was evacuated for 2 min and refilled with CO. The flask was allowed to attain room temperature and the solution was stirred for 4 h. The volatile materials were removed under vacuum and the residue was washed thoroughly with pentane (3 × 15 mL). Compounds **7a, 7b**, and **8b** were analyzed without further purification due to the low crystallinity of the products. Compound **8a** was crystallized from an Et_2O solution layered with pentane and stored at room temperature. Yield of **8a**: 164 mg, 74% of a yellow solid.

 This journal is © The Royal Society of Chemistry 2011

Published on 27 April 2011. Downloaded by University of Chicago on 30/10/2014 19:42:54.

[(BDI)(η²-OC(Me)(PEt$_3$))Nb(N^{t}Bu)][B(C$_6$F$_5$)$_4$] (7a)

^{1}H NMR (500 MHz, C$_6$H$_5$F/10% C$_6$D$_6$, 298 K), major isomer: δ 5.62 (s, 1H, *H*C(C(Me)NAr)$_2$), 3.27 (br m, 2H, C*H*Me$_2$), 2.44 (br m, 2H, C*H*Me$_2$), 1.83 (s, 6H, HC(C(*Me*)NAr)$_2$), 1.17 (s, 9H, ^{t}Bu), 0.86 (t, 9H, P*Et*$_3$), 0.62 (m, 6H, P*Et*$_3$). ^{1}H NMR (500 MHz, C$_6$H$_5$F/10% C$_6$D$_6$, 298 K), minor isomer: δ 5.70 (s, 1H, *H*C(C(Me)NAr)$_2$), 3.00 (sept, 1H, C*H*Me$_2$), 2.84 (sept, 1H, C*H*Me$_2$), 2.72 (sept, 1H, C*H*Me$_2$), the remainder of the spectrum could not be positively identified. Ratio or major to minor isomer 6.4 : 1. ^{13}C{^{1}H} NMR (125.8 MHz, C$_6$H$_5$F/10% C$_6$D$_6$, 298 K): δ 86.76 (d, $^1J_{CP}$ = 55.6 Hz, major isomer), 78.80 (d, $^1J_{CP}$ = 53.2 Hz, minor isomer). ^{31}P{^{1}H} NMR (202.5 MHz, C$_6$H$_5$F/10% C$_6$D$_6$, 298 K): δ 36.00 (br s, $\Delta\nu_{1/2}$ = 286 Hz), major isomer), 39.10 (d, $^1J_{CP}$ = 53.3 Hz, minor isomer).

[(BDI)(η²-OC(Me)(PCy$_3$))Nb(N^{t}Bu)][B(C$_6$F$_5$)$_4$] (7b)

^{1}H NMR (400 MHz, C$_6$H$_5$F/10% C$_6$D$_6$): δ 5.62 (s, 1H, *H*C(C(Me)NAr)$_2$), 3.60 (sept, 1H, C*H*Me$_2$), 3.29 (sept, 1H, C*H*Me$_2$), 2.60 (sept, 1H, C*H*Me$_2$), 2.51 (sept, 1H, C*H*Me$_2$), the remainder of the spectrum could not be positively identified due to broad, overlapping Cy signals. ^{13}C{^{1}H} NMR (100.61 MHz, C$_6$H$_5$F/10% C$_6$D$_6$): δ 89.75 (d, $^1J_{CP}$ = 53.4 Hz). ^{31}P{^{1}H} NMR (161.98 MHz, C$_6$H$_5$F/10% C$_6$D$_6$): δ 33.86 (d, $^1J_{CP}$ = 53.3 Hz).

[(BDI)(η²-OC(Me)(PEt$_3$))Ta(N^{t}Bu)][B(C$_6$F$_5$)$_4$] (8a)

^{1}H NMR (400 MHz, C$_6$H$_5$Cl/10% C$_6$D$_6$, 298 K), major isomer: δ 5.68 (s, 1H, *H*C(C(Me)NAr)$_2$), 3.52 (br m, 2H, C*H*Me$_2$), 2.40 (br m, 2H, C*H*Me$_2$), 1.82 (s, 3H, HC(C(*Me*)NAr)$_2$), 1.77 (s, 3H, HC(C(*Me*)NAr)$_2$), 1.31 (d, 3H, CH*Me*$_2$), 1.26 (d, 3H, CH*Me*$_2$), 1.19 (m, 12H), 1.14 (m, 15H), 1.00 (m, 3H), 0.86 (t, 9H, P*Et*$_3$), 0.61 (m, 6H, P*Et*$_3$). ^{1}H NMR (400 MHz, C$_6$H$_5$Cl/10% C$_6$D$_6$, 298 K), minor isomer: δ 5.68 (s, 1H, *H*C(C(Me)NAr)$_2$), 3.21 (sept, 1H, C*H*Me$_2$), 3.09 (sept, 1H, C*H*Me$_2$), 3.00 (sept, 1H, C*H*Me$_2$), 2.27 (sept, 1H, C*H*Me$_2$), 1.89 (s, 3H, HC(C(*Me*)NAr)$_2$), 1.66 (s, 3H, HC(C(*Me*)NAr)$_2$), the remaining signals could not be positively identified due to overlap with the major isomer. ^{13}C{^{1}H} NMR (100.61 MHz, C$_6$H$_5$F/10% C$_6$D$_6$, 298 K): δ 93.68 (d, $^1J_{CP}$ = 56.3 Hz, major isomer), 84.72 (d, $^1J_{CP}$ = 50.3 Hz, minor isomer). ^{31}P{^{1}H} NMR (161.98 MHz, C$_6$H$_5$F/10% C$_6$D$_6$, 298 K): δ 36.9 (br d, $^1J_{CP}$ = 56 Hz, major isomer), 41.12 (d, $^1J_{CP}$ = 50.3 Hz, minor isomer). ^{1}H NMR (400 MHz, C$_6$H$_5$Cl/10% C$_6$D$_6$, 343 K): δ 5.75 (s, 1H, *H*C(C(Me)NAr)$_2$), 3.59 (sept, 1H, C*H*Me$_2$), 2.47 (sept, 1H, C*H*Me$_2$), 2.46 (m, 2H, C*H*Me$_2$), 1.90 (s, 3H, HC(C(*Me*)NAr)$_2$), 1.84 (s, 3H, HC(C(*Me*)NAr)$_2$), 1.52 (br s, 3H), 1.42 (br s, 3H), 1.29 (d, 3H), 1.24 (d, 3H), 1.15 (m, 21H), 1.01 (d, 3H), 0.92 (d, 3H), 0.69 (m, 6H, P*Et*$_3$). ^{13}C{^{1}H} NMR (125.8 MHz, C$_6$H$_5$Cl/10% C$_6$D$_6$, 343 K): δ 93.62 (d, $^1J_{CP}$ = 53.8 Hz). ^{31}P{^{1}H} NMR (202.5 MHz, C$_6$H$_5$Cl/10% C$_6$D$_6$, 343 K): δ 36.80 (br d, $^1J_{CP}$ = 54 Hz). Anal. Calcd for C$_{65}$H$_{68}$BF$_{20}$N$_3$OPTa: C, 51.70; H, 4.54; N, 2.78. Found: C, 51.43, H 4.16; N, 3.13.

[(BDI)(η²-OC(Me)(PCy$_3$))Ta(N^{t}Bu)][B(C$_6$F$_5$)$_4$] (8b)

^{1}H NMR (400 MHz, C$_6$H$_5$F/10% C$_6$D$_6$): δ 5.71 (s, 1H, *H*C(C(Me)NAr)$_2$), 3.67 (sept, 1H, C*H*Me$_2$), 3.61 (sept, 1H, C*H*Me$_2$), 2.61 (sept, 1H, C*H*Me$_2$), 2.41 (sept, 1H, C*H*Me$_2$), the remainder of the spectrum could not be positively identified due to broad, overlapping Cy signals. ^{13}C{^{1}H} NMR (100.61 MHz, C$_6$H$_5$F/10% C$_6$D$_6$): δ 98.74 (d, $^1J_{CP}$ = 48.5 Hz). ^{31}P{^{1}H} NMR (161.98 MHz, C$_6$H$_5$F/10% C$_6$D$_6$): δ 32.65 (d, $^1J_{CP}$ = 48.6 Hz).

[(BDI)(η²-XylN═CMe)Nb(N^{t}Bu)][B(C$_6$F$_5$)$_4$] (9)

XylNC (15.9 mg, 0.12 mmol) in Et$_2$O (3 mL) was added dropwise to a stirred solution of **2a** (156 mg, 0.12 mmol) in Et$_2$O (7 mL) at room temperature. The solution immediately turned dark red, then golden yellow after a few seconds. After 5 min at room temperature, the volatile materials were removed under vacuum and the resulting pale orange solid was washed thoroughly with pentane (2 × 10 mL). The residual solvent was removed under vacuum to yield a pale yellow powder. Yield: 152 mg, 88%. ^{1}H NMR (500 MHz, C$_6$D$_5$Cl, 298 K): δ 5.72 (s, *H*C(C(Me)NAr)$_2$ of major isomer), 5.71 (s, *H*C(C(Me)NAr)$_2$ of minor isomer). ^{1}H NMR (500 MHz, C$_6$D$_5$Cl, 343 K): δ 7.3–6.9 (m, Ar), 5.74 (s, 1H, *H*C(C(Me)NAr)$_2$), 3.05 (br m, 2H, C*H*Me$_2$), 2.47 (br m, 2H, C*H*Me$_2$), 2.17 (br s, 3H, Xyl), 2.06 (br s, 3H, Xyl), 1.87 (br s, 3H, HC(C(*Me*)NAr)$_2$), 1.78 (br s, 3H, HC(C(*Me*)NAr)$_2$), 1.50 (br s, 3H, XylN═C*Me*), 1.3–0.6 (br m, CH*Me*$_2$ and ^{t}Bu). Anal. Calcd for C$_{67}$H$_{62}$BF$_{20}$N$_4$Nb: C, 57.20; H, 4.44; N, 3.98. Found: C, 57.49, H 4.68; N, 3.91. IR (KBr, nujol, cm^{-1}): 1642 (m, ν_{CN} iminoacyl).

[(BDI)(PhMe$_2$CO)Nb(N^{t}Bu)][B(C$_6$F$_5$)$_4$] (11)

Acetophenone (14.2 μL, 0.12 mmol) was added by syringe to a solution of **2a** (156 mg, 0.12 mmol) in Et$_2$O (5 mL). The color of the solution lightened slightly, and the solution was stirred for 30 min. A pale yellow solid was obtained by removing the solvent *in vacuo* and washing the resulting oil with several portions of pentane, followed by removing the residual solvent under vacuum. Yield: 156 mg, 91%. ^{1}H NMR (400 MHz, C$_6$D$_5$Cl): δ 7.06–7.30 (m, 11H, Ar), 6.19 (s, 1H, *H*C(C(Me)NAr)$_2$), 2.34 (sept, 2H, ^{i}Pr-C*H*), 2.05 (sept, 2H, ^{i}Pr-C*H*), 1.95 (s, 6H, HC(C(*Me*)NAr)$_2$), 1.66 (s, 6H, *Me*$_2$C(Ph)ONb), 1.22 (d, 6H, ^{i}Pr-*Me*), 1.13 (d, 6H, ^{i}Pr-*Me*), 0.94 (d, 6H, ^{i}Pr-*Me*), 0.72 (d, 6H, ^{i}Pr-*Me*), 0.68 (s, 9H, ^{t}Bu). ^{13}C NMR (125 MHz, C$_6$D$_5$Cl): δ 172.07 (HC(*C*(Me)NAr)$_2$), 149.50 (*C*$_6$F$_5$), 147.60 (*C*$_6$F$_5$), 146.57 (Ar), 141.76 (Ar), 140.18 (Ar), 139.87 (Ar), 137.50 (*C*$_6$F$_5$), 135.70 (*C*$_6$F$_5$), 129.58 (Ar), 128.85 (Ar), 125.17 (Ar), 124.61 (Ar), 123.99 (Ar), 99.35 (H*C*(C(Me)NAr), 86.66 (O*C*Me$_2$Ph), 73.95 (^{t}Bu, C$_\alpha$), 32.26 (OC*Me*$_2$Ph), 30.81 (^{t}Bu, C$_\beta$), 30.00 (*C*HMe$_2$), 28.68 (*C*HMe$_2$), 25.37 (HC(C(*Me*)NAr)$_2$), 24.29 (CH*Me*$_2$), 24.23 (CH*Me*$_2$), 23.76 (CH*Me*$_2$), 23.71 (CH*Me*$_2$). ^{19}F NMR (376.5 MHz, C$_6$D$_5$Cl): δ –130.7 (s, *o*-F), –161.43 (t, *m*-F), –165.24 (t, *p*-F). Anal. Calcd for C$_{66}$H$_{61}$BF$_{20}$N$_3$NbO: C, 56.79; H, 4.40; N, 3.01. Found: C, 56.94, H 4.58; N, 2.89.

[(BDI)(PhMe$_2$CO)Ta(N^{t}Bu)][B(C$_6$F$_5$)$_4$] (12)

Compound **12** was prepared following the procedure given for **11**, using 120 mg (0.088 mmol) of **6**, 10.3 µL of acetophenone, and fluorobenzene as the solvent instead of Et$_2$O. The product was isolated as an orange powder. Yield: 123 mg, 94%. ^{1}H NMR (500 MHz, C$_6$H$_5$F/10% C$_6$D$_6$, 298 K): δ 7.25–7.10 (m, 11H, Ar), 6.15 (s, 1H, *H*C(C(Me)NAr)$_2$), 2.37 (sept, 2H, C*H*Me$_2$), 2.14 (sept, 2H, C*H*Me$_2$), 1.94 (s, 6H, HC(C(*Me*)NAr)$_2$), 1.65 (s, 6H, Ph*Me*$_2$COTa), 1.15 (d, 6H, CH*Me*$_2$), 1.11 (d, 6H, CH*Me*$_2$), 0.92 (d, 6H, CH*Me*$_2$), 0.71 (d, 6H, CH*Me*$_2$), 0.65 (s, 9H, ^{t}Bu). ^{13}C NMR (125 MHz, C$_6$H$_5$F/10% C$_6$D$_6$): δ 175.2 (HC(*C*(Me)NAr)$_2$), 150.4

Published on 27 April 2011. Downloaded by University of Chicago on 30/10/2014 19:42:54.

(C_6F_5), 148.5 (C_6F_5), 147.2 (Ar), 141.7 (Ar), 141.5 (Ar), 141.1 (Ar), 138.2 (C_6F_5), 136.3 (C_6F_5), 130.4 (Ar), 129.5 (Ar), 128.6 (Ar), 125.9 (Ar), 125.3 (Ar), 124.7 (Ar), 98.8 (H*C*(C(Me)NAr), 87.5 (O*C*Me$_2$Ph), 69.9 (^{t}Bu, C$_\alpha$), 32.7 (^{t}Bu, C$_\beta$), 32.7 (OC*Me*$_2$Ph), 30.7 (*C*HMe$_2$), 29.3 (*C*HMe$_2$), 25.8, 25.2, 24.7, 24.2, 24.1. Anal. Calcd for $C_{66}H_{61}BF_{20}N_3OTa$: C, 53.42; H, 4.14; N, 2.83. Found: C, 53.59, H 4.14; N, 2.94.

[(BDI){κ²-*N*$_2$-MeC(NCy)$_2$}Nb(N^{t}Bu)][B(C$_6$F$_5$)$_4$] (13)

A solution of CyN═C═NCy (20 mg, 0.08 mmol) in chlorobenzene (2 mL) was added to a solution of **2a** (104 mg, 0.08 mmol) in chlorobenzene (6 mL). The solution turned from yellow–orange to deep red–orange over 3 h, after which time the volatile materials were removed under vacuum. The resulting red–orange oil solidified after washing with pentane (3 × 10 mL) and removing the residual solvent under vacuum. Yield: 102 mg, 84%. ^{1}H NMR (500 MHz, C_6D_5Cl): δ 7.25–7.00 (m, 6H, Ar), 5.90 (s, 1H, *H*C(C(Me)NAr)$_2$), 3.22 (sept, 2H, C*H*Me$_2$), 2.64 (pent, 2H, NC*H*), 2.26 (sept, 2H, C*H*Me$_2$), 1.82 (s, 6H, HC(C(*Me*)NAr)$_2$), 1.82 (s, 3H, NC(*Me*)N), 1.5 (br m, 8H, Cy), 1.20 (d, 6H, CH*Me*$_2$), 1.14 (d, 6H, CH*Me*$_2$), 1.14 (s, 9H, ^{t}Bu), 1.10 (d, 6H, CH*Me*$_2$), 1.07 (br m, 8H, Cy), 0.87 (d, 6H, CH*Me*$_2$), 0.80 (br m, 4H, Cy). ^{13}C{^{1}H} NMR (125.7 MHz, C_6D_5Cl): δ 185.6, 172.6, 148.8, 147.7, 142.9, 142.1, 140.7, 137.5, 135.5, 129.0, 124.8, 108.8, 74.5, 60.0, 34.1, 32.1, 31.7, 29.3, 27.4, 26.0, 25.5, 25.0, 24.7, 24.6, 23.1, 22.4, 20.6, 13.9. IR: $\nu_{C=N}$ (cm^{-1}) = 1643 (amidinate), 1513 (BDI). Anal. Calcd for $C_{71}H_{75}BF_{20}N_5Nb$: C, 57.54; H, 5.10; N, 4.73. Found: C, 57.34, H 5.22; N, 5.10.

[(BDI)(^{t}BuMeC═N)Nb(N^{t}Bu)][B(C$_6$F$_5$)$_4$] (14)

^{t}BuCN (13.4 μL, 0.12 mmol) was added by syringe to a solution of **2a** (156 mg, 0.12 mmol) in Et$_2$O (10 mL). The solution immediately turned red–orange. After 3 h at room temperature, the solution was concentrated under vacuum to *ca.* 2 mL, at which point an orange microcrystalline material precipitated from the solution. The solid was collected following isolation from the mother liquor by filtration and removal of the residual solvent under vacuum. Yield: 137 mg, 83%. ^{1}H NMR (500 MHz, C_6D_5Cl, 298 K): δ 7.1–6.8 (m, Ar), 5.49 (br s, 1H, *H*C(C(Me)NAr)$_2$), 2.62 (br m, 2H, C*H*Me$_2$), 2.43 (br m, 2H, C*H*Me$_2$), 1.56 (br s, 6H, HC(C(*Me*)NAr)$_2$), 1.31 (s, 3H, ^{t}Bu*Me*C═N), 1.09 (br s, 12 H, CH*Me*$_2$), 1.02 (br s, 9H, ^{t}Bu), 0.89 (br s, 12H, CH*Me*$_2$), 0.71 (s, 9H, ^{t}Bu). ^{1}H NMR (500 MHz, $C_6H_5Cl(C_6D_6)$, 343 K): (Aryl resonances were obscured by solvent peaks) δ 5.69 (s, 1H, *H*C(C(Me)NAr)$_2$), 2.55 (br s, 2H, C*H*Me$_2$), 2.43 (br s, 2H, C*H*Me$_2$), 1.74 (s, 6H, HC(C(*Me*)NAr)$_2$), 1.34 (s, 3H, ^{t}Bu*Me*C═N), 1.18 (d, 12H, CH*Me*$_2$), 1.10 (br s, 6H, CH*Me*$_2$), 0.96 (br s, 6H, CH*Me*$_2$), 0.86 (s, 9H, ^{t}Bu), 0.85 (s, 9H, ^{t}Bu). ^{1}H NMR (500 MHz, C_6D_5Cl, 223 K): δ 5.63 (s, *H*C(C(Me)NAr)$_2$ of minor isomer), 5.43 (s, *H*C(C(Me)NAr)$_2$ of major isomer). The remaining signals were still unresolved at this temperature. Ratio of major : minor isomers = 2.5. Anal. Calcd for $C_{63}H_{62}BF_{20}N_4Nb$: C, 55.68; H, 4.60; N, 4.12. Found: C, 55.80, H 4.89; N, 4.50.

[(BDI)(Ph$_3$SiO)Nb(N^{t}Bu)][B(C$_6$F$_5$)$_4$] (15)

Ph_3SiOH (20.3 mg, 0.07 mmol) was dissolved in fluorobenzene (2 mL) and added to a solution of **2a** (93 mg, 0.07 mmol) in fluorobenzene at room temperature. The solution effervesced as the color lightened to pale yellow. After 10 min, the volatile materials were removed under vacuum, and the resulting oil was washed with pentane (3 × 5 mL) and dried under vacuum to yield a pale yellow powder. Yield: 98 mg, 87%. ^{1}H NMR (500 MHz, C_6H_5F/10% C_6D_6): δ 7.70 (m, 6H, Si*Ph*$_3$), 7.30 (m, 9H, Si*Ph*$_3$), 6.46 (s, 1H, *H*C(C(Me)NAr)$_2$), 2.38 (sept, 2H, C*H*Me$_2$), 2.09 (s, 6H, HC(C(*Me*)NAr)$_2$), 1.94 (sept, 2H, C*H*Me$_2$), 1.18 (d, 6H, CH*Me*$_2$), 0.96 (d, 6H, CH*Me*$_2$), 0.89 (d, 6H, CH*Me*$_2$), 0.72 (s, 9H, ^{t}Bu), 0.32 (d, 6H, CH*Me*$_2$). ^{13}C{^{1}H} NMR (125.7 MHz, C_6H_5F/10% C_6D_6, 298 K): δ 172.9, 142.3, 141.5, 140.4, 135.4, 134.7, 131.5, 129.1, 125.8, 125.2, 99.4, 76.2, 31.1, 31.0, 29.5, 26.1, 24.8, 24.5, 24.2, 23.6. ^{29}Si NMR (99.4 MHz, C_6H_5F/10% C_6D_6): δ −13.36. Anal. Calcd for $C_{75}H_{65}BF_{20}N_3NbOSi$: C, 58.64; H, 4.27; N, 2.74. Found: C, 58.80, H 4.44; N, 3.02.

[(BDI)(Ph$_3$SiO)Ta(N^{t}Bu)][B(C$_6$F$_5$)$_4$] (16)

Compound **16** was prepared following the procedure given for **15**, using 100 mg (0.07 mmol) of **6** and 20.3 mg (0.07 mmol) of Ph_3SiOH. The product was obtained as a white powder. Yield: 120 mg, 91%. ^{1}H NMR (500 MHz, C_6H_5Cl/10% C_6D_6): δ 7.70 (m, 6H, Si*Ph*$_3$), 7.33 (m, 9H, Si*Ph*$_3$), 6.43 (s, 1H, *H*C(C(Me)NAr)$_2$), 2.37 (sept, 2H, C*H*Me$_2$), 2.07 (s, 6H, HC(C(*Me*)NAr)$_2$), 1.93 (sept, 2H, C*H*Me$_2$), 1.18 (d, 6H, CH*Me*$_2$), 0.95 (d, 6H, CH*Me*$_2$), 0.88 (d, 6H, CH*Me*$_2$), 0.70 (s, 9H, ^{t}Bu), 0.25 (d, 6H, CH*Me*$_2$). ^{13}C{^{1}H} NMR (125.7 MHz, C_6H_5F/10% C_6D_6, 298 K): δ 175.3, 141.9, 141.4, 140.9, 135.4 134.4, 131.6, 129.2, 128.9, 125.9, 125.2, 99.0, 71.0 (^{t}Bu, C$_\alpha$), 32.5 (^{t}Bu, C$_\beta$), 31.2, 29.4, 26.1, 25.3, 24.5, 24.2, 23.6. ^{29}Si NMR (99.4 MHz, C_6H_5F/10% C_6D_6): −12.15. Anal. Calcd for $C_{75}H_{65}BF_{20}N_3OSiTa$: C, 55.46; H, 4.03; N, 2.59. Found: C, 55.65, H 4.26; N, 2.57.

Polymerization of ethylene with 2b

A solution of **2b** (21.2 mg, 0.019 mmol) in 15 mL of C_6H_5Cl was added to a 100 mL Schlenk flask. The solution was frozen, and the headspace was evacuated and replaced with an atmosphere of ethylene (85 mL, 3.5 mmol). The flask was sealed and allowed to warm to room temperature. The solution was stirred for 12 h, over which time a solid deposited. Methanol (5 mL) was added, and the solid was collected on a frit, washed with $HF_{(aq)}$ (0.5 M, 10 mL) then water (50 mL) and dried under vacuum to give a white solid. Yield: 95 mg, 92%. M.p. 122 °C.

Results and discussion

Synthesis and characterization of four-coordinate niobium cations

Published synthetic routes to early-metal alkyl cations involve alkyl or halide group abstraction, alkyl group protonolysis, oxidation of *d*-electron containing species, or oxidation of metal–carbon bonds. In the systems described here, we found alkyl group abstraction and alkyl group protonolysis reactions to be the most effective.

Within the category of alkyl anion group removal, several routes were available for generating stable, monomeric cations from our previously described dimethyl complex (BDI)Me$_2$Nb(N^{t}Bu) (**1**). The complex [(BDI)MeNb(N^{t}Bu)][B(C$_6$F$_5$)$_4$] (**2a**) was prepared by addition of a solution of either [(Et$_2$O)$_2$H][B(C$_6$F$_5$)$_4$] in Et$_2$O or [Ph$_3$C][B(C$_6$F$_5$)$_4$] in chlorobenzene to a solution of **1** in Et$_2$O

 This journal is © The Royal Society of Chemistry 2011

Published on 27 April 2011. Downloaded by University of Chicago on 30/10/2014 19:42:54.

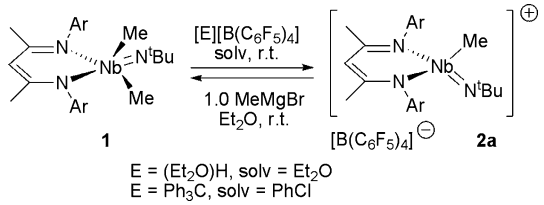

Scheme 1

or chlorobenzene, respectively (Scheme 1). Reaction with either reagent occurs within seconds at room temperature and results in a color change from pale yellow to golden yellow. Use of Jutzi's acid, $[(Et_2O)_2H][B(C_6F_5)_4]$,[41] was found to be the preferable method because of the ease of preparation of the acid from $KB(C_6F_5)_4$, its crystallinity, and its formation of volatile by-products (Et_2O and CH_4) on reaction with a methide group. The solution rapidly effervesces in the case of $[(Et_2O)_2H][B(C_6F_5)_4]$, and 1,1,1-triphenylethane may be observed by ^{1}H NMR when $[Ph_3C][B(C_6F_5)_4]$ is used.

A ^{1}H NMR spectrum of the product taken in chlorobenzene-d_5 indicates that the molecule has averaged C_s symmetry in solution. The spectrum has sharp lines at room temperature, and the observed symmetry in solution does not change on heating or cooling (+70/−40 °C) the sample in the NMR probe. The spectrum has one singlet at 1.01 ppm corresponding to the remaining Nb-bound methyl group, and a ^{19}F NMR spectrum of the crystallized product displays the expected resonances for the $[B(C_6F_5)_4]^-$ group. The resonance due to the Nb–CH_3 carbon in the ^{13}C NMR spectrum is not shifted appreciably from the signal for the two Nb–Me groups of the starting material, but the $\Delta\delta_{\alpha\beta}$ value for **2a** increased to 45.3, compared to 35.1 (*avg.*) for the neutral dimethyl,[42] suggesting that the imido nitrogen of **2a** is less shielded than that of **1**.[25] Since both compounds **1** and **2a** have orbitals available that can accommodate Nb–N triple bonding (1σ, 2π),[48] this increase in the $\Delta\delta_{\alpha\beta}$ value indicates a change in the electrophilicity of the metal center, not simply an orbital rehydridization about the metal center to accommodate formerly symmetry-forbidden π-bonding from the imido nitrogen. Used in this qualitative sense for comparing two closely-related complexes, the $\Delta\delta_{\alpha\beta}$ values provide a useful point of comparison of the relative electron deficiency of the metal centers.[49]

The product is insoluble in pentane and benzene and fully soluble in ethers and haloarenes, which is consistent with a molecule of considerably higher polarity than that of the starting material. The formation of a dimer in solution is unlikely considering the build-up of charge required by dimerization, and notably, the high $\Delta\delta_{\alpha\beta}$ falls outside the range observed for amido-type ^{t}Bu groups.[50] Derivatization of **2a** by addition of 1.0 equiv of MeMgBr to a solution of **2a** in Et_2O cleanly reforms **1**, and while the dimethyl complex decomposes thermally, compound **2a** is stable at room temperature under an inert atmosphere in the solid state, decomposing appreciably only at 75 °C in solution. These data all support the formulation of **2a** as a monomeric, ion-paired, tetrahedral methylniobium complex; a composition that was also found in the solid state.

Single crystals of **2a** were grown from Et_2O, and a crystallographic study reveals a unit cell containing the niobium cation, $B(C_6F_5)_4$ anion (Fig. 1) and four Et_2O of crystallization.

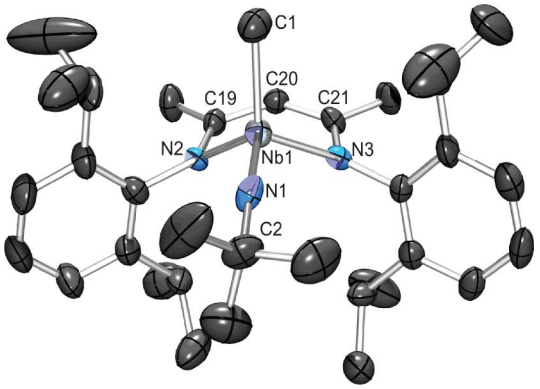

Fig. 1 Molecular structure of the cationic portion of **2a** as determined by a single crystal X-ray diffraction study. The hydrogen atoms, the two co-crystallized molecules of Et_2O, and the $B(C_6F_5)_4$ anion were omitted for clarity; the thermal ellipsoids were set at the 50% probability level. Selected bond lengths (Å): Nb(1)–C(1) 2.163(5), Nb(1)–N(1) 1.737(4), Nb(1)–N(2) 2.038(4), Nb(1)–N(3) 2.036(4), N(2)–C(19) 1.341(6), C(19)–C(20) 1.419(7), C(20)–C(21) 1.405(7), N(3)–C(21) 1.354(6). Selected bond angles (°): N(1)–Nb(1)–N(3) 108.22(18), N(1)–Nb(1)–N(2) 108.59(19), N(3)–Nb(1)–N(2) 96.13(16), N(1)–Nb(1)–C(1) 108.0(2), N(3)–Nb(1)–C(1) 116.0(2), N(2)–Nb(1)–C(1) 119.13(19).

The cationic Nb center has a distorted tetrahedral geometry, constrained by the bite angle of the BDI ligand (N(2)–Nb(1)–N(3) = 96.11°), which has opened up considerably from that of **1** (N(2)–Nb(1)–N(3) = 83.33°). The structural changes induced by the lower coordination number and the cationic charge at the metal center are reflected by a contracted Nb–Me bond length of 2.164 Å compared to that in **1** (2.177 and 2.187 Å) and a shorter Nb–N_{imido} bond length (1.736 Å *vs.* 1.777 Å for **1**). The non-crystallographically imposed local mirror symmetry of the cation results in statistically indistinguishable Nb–N_{BDI} bond lengths of 2.036(4) and 2.038(4) Å, whereas the *trans*-influence of the imido group in complex **1** lengthens the Nb–N_{BDI} bond for the nitrogen *trans* to the imido to 2.357 Å, compared to 2.136 Å for the equatorial Nb–N_{BDI} bond.

A related cationic complex was prepared by addition of a chlorobenzene solution containing 1.0 equiv of $B(C_6F_5)_3$ to a solution of **1** in chlorobenzene, resulting in methide group abstraction to form [(BDI)MeNb(N^{t}Bu)][$MeB(C_6F_5)_3$] (**2b**, Scheme 2). A ^{1}H NMR spectrum of the product in chlorobenzene-d_5 revealed that the transition metal-based portion of the molecule has an identical composition to that in **2a**. The boron-bound methyl group resonates at 1.25 ppm, and the ^{19}F NMR spectrum reveals $\Delta(mF - pF)$ = 2.4 ppm, indicating that on the NMR time scale the methylborate anion shows no directional interaction with the metal center.[51] The solubility of this complex (soluble in Et_2O, THF, chlorobenzene; insoluble in C_6H_6 and pentane) is similar to that of the related cationic complex **2a**, thus supporting

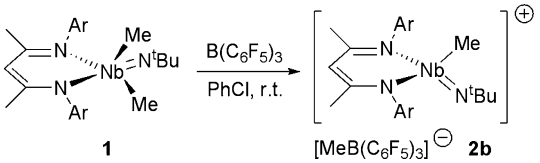

Scheme 2

Published on 27 April 2011. Downloaded by University of Chicago on 30/10/2014 19:42:54.

the formulation of **2b** as an ion-paired niobium cation with a methylborate anion.

Synthesis of tantalum dichloride, dimethyl and cationic monomethyl complexes

Due partly to the stronger bonds between Ta and the lighter p-block elements compared to the analogous Nb–p-block bonds, the chemistry of Ta has received considerably more attention than that of its lighter congener. This difference in reactivity between the 4d and 5d metals has been used for forming stable 5d metal analogs of 4d metal complexes that are too reactive to be investigated. Thus, for comparison of the Nb chemistry with the better-known Ta chemistry, we prepared the dichloride, dimethyl, and cationic monomethyl Ta complexes analogous to the Nb complexes (BDI)pyCl$_2$Nb(N^{t}Bu) (**3**), **1**, and **2a**, respectively.

Synthesis of the dichlorotantalum complex (BDI)-pyCl$_2$Ta(N^{t}Bu) (**4**, Scheme 3) proceeded in a manner similar to that of the analogous niobium complex **3**,[42] though heating the solution to reflux for 12 h was required to drive the reaction to completion. The product was crystallized from a saturated Et$_2$O solution at −80 °C, although in lower yields than for **3**. The crystalline material obtained from this process quickly desolvates, affording a bright yellow powder after drying under vacuum. The ^{1}H NMR spectrum of **4** has features similar to those of **3**, displaying averaged C$_s$ symmetry with peak broadening due to reversible pyridine dissociation in solution.

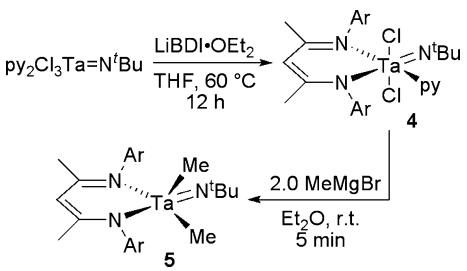

Scheme 3

Crystals suitable for X-ray analysis were grown from hot hexane (+65/+20 °C). The molecular structure is illustrated in Fig. 2, with selected metric parameters reproduced in the caption. The metal center has a distorted octahedral geometry, with the two axial chlorines angled toward the pyridine ligand (Cl(1)–Ta(1)–Cl(2) = 160.85°). Due to the effect of the lanthanide contraction, the bond lengths about the metal center are similar to those for the analogous Nb complex (**3**) described previously (maximum deviation <1.2%).

The dimethyl tantalum complex was synthesized by addition of 2.0 equiv of MeMgBr to a solution of **4** in Et$_2$O. The dimethyl product (BDI)Me$_2$Ta(N^{t}Bu) (**5**, Scheme 3) was crystallized from a saturated pentane solution, yielding pale yellow blocks suitable for crystallographic analysis. The overall geometry of **5** (Fig. 3) is similar to that of **1**, being trigonal bipyramidal (τ = 0.71)[52] with equatorial methyl groups (Ta(1)–C(1) = 2.194 Å; Ta(1)–C(2) = 2.172 Å), an axial imido ligand (d(Ta(1)–N(1)) = 1.779 Å), and a BDI ligand spanning axial and equatorial coordination sites.

The crystallographic data fit more accurately with a model that incorporates 15% occupancy of chlorine near the C(1) site and

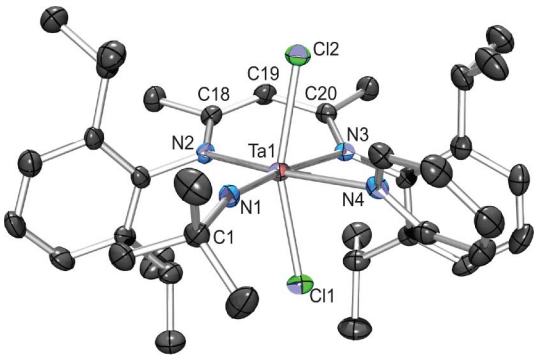

Fig. 2 Molecular structure of **4** as determined by a single crystal X-ray diffraction study. The hydrogen atoms were omitted for clarity; the thermal ellipsoids were set at the 50% probability level. Selected bond lengths (Å): Ta(1)–N(1) 1.784(2), Ta(1)–N(2) 2.108(2), Ta(1)–N(3) 2.392(2), Ta(1)–N(4) 2.350(2), Ta(1)–Cl(1) 2.4128(7), Ta(1)–Cl(2) 2.3993(7), N(2)–C(18) 1.378(4), C(18)–C(19) 1.370(4), C(19)–C(20) 1.426(4), N(3)–C(20) 1.324(4). Selected bond angles (°): Ta(1)–N(1)–C(1) 164.9(2), Cl(1)–Ta(1)–Cl(2) 160.85(3), N(1)–Ta(1)–N(3) 174.34(9), N(2)–Ta(1)–N(4) 173.32(8), N(2)–Ta(1)–N(3) 83.59(9).

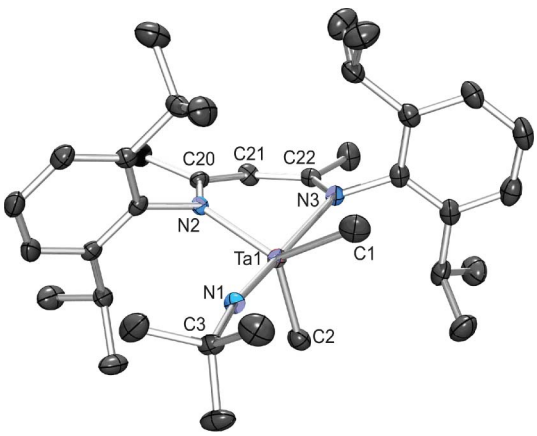

Fig. 3 Molecular structure of **5** as determined by a single crystal X-ray diffraction study. The hydrogen atoms and Cl(1) were omitted for clarity; the thermal ellipsoids were set at the 50% probability level. Selected bond lengths (Å): Ta(1)–C(1) 2.193(14), Ta(1)–C(2) 2.172(4), Ta(1)–N(1) 1.779(3), Ta(1)–N(2) 2.119(3), Ta(1)–N(3) 2.347(3), N(2)–C(20) 1.362(5), C(20)–C(21) 1.381(5), C(21)–C(22) 1.405(5), N(3)–C(22) 1.317(5). Selected bond angles (°): N(2)–Ta(1)–C(2) 112.57(14), N(2)–Ta(1)–C(1) 129.6(4), C(2)–Ta(1)–C(1) 115.7(4), N(1)–Ta(1)–N(3) 172.17(12), N(2)–Ta(1)–Cl(1) 136.3(8), C(3)–N(1)–Ta(1) 168.5(3).

in place of the C(1) methyl group (d(Ta(1)–Cl(1)) = 2.379 Å), indicating that complex **5** has co-crystallized with the methyl chloride complex (BDI)ClMeTa(N^{t}Bu). The formation of this compound is assumed to occur *via* addition of an insufficient amount of MeMgBr. Interestingly, attempts at forming mixed alkyl chloride complexes in the Nb system failed.[42]

In contrast to the behavior of the Nb complex **1**, reaction of **5** with B(C$_6$F$_5$)$_3$ failed to yield the homologous methyltantalum cation, presumably due to the stronger Ta–Me bond compared to that in the Nb system. Nevertheless, on reaction of a slight excess of **5** with either [Ph$_3$C][B(C$_6$F$_5$)$_4$] or [(Et$_2$O)$_2$H][B(C$_6$F$_5$)$_4$] in fluorobenzene, the solution turned golden yellow, and when the protic acid was used the solution rapidly effervesced.

 This journal is © The Royal Society of Chemistry 2011

Published on 27 April 2011. Downloaded by University of Chicago on 30/10/2014 19:42:54.

Removal of the volatile materials under vacuum followed by multiple pentane washes yielded the cationic complex [(BDI)MeTa(N^{t}Bu)][B(C$_6$F$_5$)$_4$] (**6**, Scheme 4) in good yield and high purity.

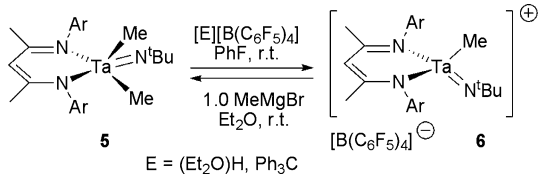

Scheme 4

The ^{1}H NMR spectrum of **6** closely resembles that of **2a**, which indicates local, averaged C_s symmetry for the cation in solution. The chemical shift of the Ta–Me group at 0.83 ppm is shifted upfield from that for **2a**, but like **2a**, the ^{13}C{^{1}H} NMR spectrum reveals a large $\Delta\delta_{\alpha\beta}$ value of 39.2, indicative of increased donation of electron density from the imido nitrogen to the metal center. Solutions of **6**, like **2a**, are stable in the presence of the parent dimethyl complex, and addition of 1.0 equiv of MeMgBr to a solution of **6** in Et$_2$O regenerated the dimethyl complex **5** in quantitative yield. The stability of **6** in Et$_2$O is limited, and attempts at crystallizing the product from Et$_2$O/pentane resulted in a crystalline mixture of **6** and another unidentified product that may have incorporated Et$_2$O, based on NMR analysis.

Insertion of CO and XylNC

We were initially interested in carbonylating **2a** and **6** to form cationic acyl complexes as an extension of our previous work studying the carbonylation pathways available to the dimethyl complex (BDI)Me$_2$Nb(N^{t}Bu) (**1**).[53] The complicated mixture of products observed on carbonylation of the **1** was attributed largely to the various reaction pathways available to the remaining niobium-bound methyl group following formation of the transient monoacyl intermediate. Accordingly, when the methyl bromide complex (BDI)MeBrNb(N^{t}Bu) was exposed to carbon monoxide, the compound cleanly inserted CO at room temperature to yield an observable monoacyl.[53] We consequently reasoned that the cationic monomethyl compounds could serve as suitable entry points into stoichiometric monoacyl chemistry and provide a powerful tool for C–C bond formation.

Surprisingly, neither **2a** nor **6** reacted with CO to yield an observable complex in solution (1 atm CO, 20 °C). NMR spectra of a solution of the cationic complexes under CO did not indicate a change in the molecular constitution of the complexes, and methylation of the material recovered from the attempted carbonylation yielded only the parent dimethyl compounds. This lack of reactivity was especially surprising considering the range of products observed upon carbonylation of **1**. Reversible carbonylation of early-metal alkyls is well-documented in the literature but has generally been observed with metallocene systems which have a limited number of vacant orbitals.[54] In these cases, the facility of the de-insertion reaction was found to depend on the donor capability of the other, non-Cp ligand.[55] In the current system, the failure of **2a** and **6** to insert CO indicates that any energetic gain in M–O bond energy (the effect widely believed to drive the formation of early-metal acyls) can be counteracted by a decrease in M–C bonding energy and by a decrease in entropy. The higher cationic charge at the metal center, shown crystallographically to result in shorter Nb–C and Nb–N$_{imido}$ bond lengths, may shift the equilibrium toward the side of free CO despite the electron deficiency at the metal center.

While NMR spectroscopic observation of a stable acyl adduct was not possible, a transient insertion product was trapped by phosphines to yield the tetrahedral Lewis base adducts of an acyl. Addition of CO to solutions of either **2a** or **6** in the presence of phosphines resulted in rapid reactions to give the phosphine-trapped acyl complexes [(BDI)(η^2-OC(Me)(PR$_2$R′))M(N^{t}Bu)][B(C$_6$F$_5$)$_4$] (**7a**, R = R′ = Et, M = Nb; **7b**, R = R′ = Cy, M = Nb; **8a**, R = R′ = Et, M = Ta; **8b**, R = R′ = Cy, M = Ta; Scheme 5). Compound **8a** was isolated as a crystalline solid in high yield, and the remaining compounds were characterized by analysis of the reaction mixture by NMR spectroscopy, which indicated that the products formed in >90% yield.

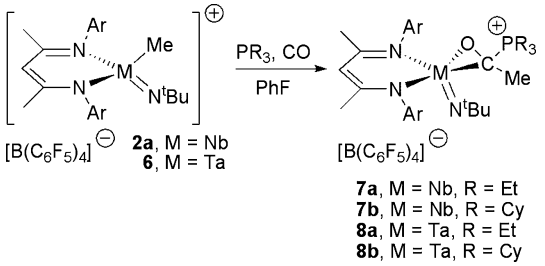

Scheme 5

The ^{13}C{^{1}H} NMR spectra obtained on samples of **7a, b** and **8a, b** synthesized with ^{13}CO exhibit doublets in the 80–100 ppm range with coupling constants (*ca.* 50 Hz) identical to those observed for doublets in the ^{31}P{^{1}H} spectrum (20–45 ppm, Tables 2 and 3). Coupling constants in this range are indicative of $^1J_{CP}$ interactions, and related acyl and silaacyl complexes exhibit similarly upfield-shifted carbon signals for the metal-bound carbon atom (relative to transition-metal acyls) and downfield-shifted phosphorus resonances (relative to the free phosphine).[56–66] These signals are indicative of the alkoxide and phosphonium character of the carbon and phosphorus atoms, respectively. Although the crystallographic data were not sufficient to fully elucidate the structure, a partial X-ray crystal structure of **8a** supports the proposed formulation of the products as the monomeric, phosphine coordinated η^2-acyl complexes (Scheme 5).

While the mechanism of this reaction has not been determined, it should be noted that, as observed with CO, no change in the ^{1}H NMR spectrum of the cation could be detected upon

Table 2 Chemical shifts (in ppm) of the signals in ^{13}C{^{1}H} and ^{31}P{^{1}H} NMR spectra corresponding to the ^{13}C labelled carbon and the phosphonium phosphorus

	Isomer 1[a]		Isomer 2[a]		343 K	
Compound	^{13}C	^{31}P	^{13}C	^{31}P	^{13}C	^{31}P
7a	86.76	36.00	78.80	39.10	—	—
7b	89.75	33.86	—	—	—	—
8a	93.68	36.9	84.72	41.12	93.62	36.80
8b	98.74	32.65	—	—	—	—

[a] Collected at 298 K.

Published on 27 April 2011. Downloaded by University of Chicago on 30/10/2014 19:42:54.

Table 3 $^{1}J_{CP}$ coupling constants (in Hz) for the signals in the $^{13}C\{^{1}H\}$ and $^{31}P\{^{1}H\}$ NMR spectra corresponding to the ^{13}C labelled carbon and the phosphonium phosphorus

	Isomer 1[a]		Isomer 2[a]		343 K	
Compound	^{13}C	^{31}P	^{13}C	^{31}P	^{13}C	^{31}P
7a	55.6	—[b,c]	53.2	53.3	—	—
7b	53.4	53.3	—	—	—	—
8a	56.3	56[c]	50.3	50.3	53.8	54(1)[c]
8b	48.5	48.6	—	—	—	—

[a] Collected at 298 K. [b] The signal appeared as a broad singlet at this temperature. [c] Precision of measurement decreased due to line broadening at these temperatures.

treatment with an excess of phosphine. Known methods for the synthesis of related compounds have been performed in a stepwise fashion, where CO addition to alkyl or silyl complexes led to isolatable acyls; subsequent reactions with phosphines generated the phosphine-coordinated (sila-)acyls.[61–62]

The electrophilicity of early-metal acyl carbons indicates that direct intermolecular addition of nucleophiles to the acyl carbons is a likely mechanism (Scheme 6, route *a*). While this could be occurring during the formation of compounds **7a, b** and **8a, b**, another possibility would be a "phosphine-first" mechanism (Scheme 6, route *b*). In this case, phosphine coordination would create a more electron-rich, pentacoordinate complex, similar to the methyl bromide complex (BDI)MeBrNb(N^{t}Bu), which has been observed to form a stable niobium acyl at room temperature.[53] CO coordination and insertion into the Ta–Me bond of the phosphine-coordinated cation would lead to an acyl complex. Subsequent phosphine migration to the acyl carbon would then furnish the phosphine trapped acyl products **7a, b** and **8a, b** in a mechanism reminiscent of methyl group migration to form the intermediate ketone adduct upon carbonylation of **1**.

Compounds **7b** and **8b** appear to form only one isomer in solution, while **7a** and **8a** form as a mixture of isomers (Fig. 4). In the latter cases, the major isomer displays considerable fluxional behavior at room temperature. Heating a solution of **8a** to 343 K causes the two isomers to interconvert rapidly on the NMR time scale, allowing for observation of a time-averaged species, as determined by monitoring the coalescence of the BDI ligand backbone methine signals. The $^{13}C\{^{1}H\}$ and $^{31}P\{^{1}H\}$ spectra of the ^{13}C-labelled compound similarly indicate that the two isomers are in rapid equilibrium relative to the NMR timescale at elevated

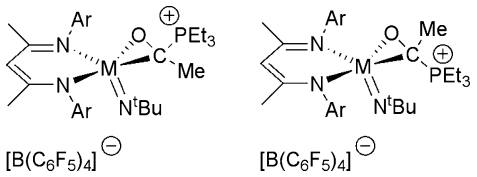

Fig. 4 Two diastereomers of **7a** (M = Nb) and **8a** (M = Ta) proposed to form on coordination of PEt_3 to the acyl carbon.

temperature, resulting in a single doublet in each spectrum. The chemical shifts of the doublets are close to the values of the major isomer observed at room temperature but have shifted slightly in the direction of the minor isomer (Tables 2 and 3).

Compared to CO insertion reactions, the insertion of isocyanides into early-metal alkyl bonds is more likely to result in stable products.[54] Accordingly, a rapid reaction (in the absence of a phosphine) was observed between 1.0 equiv of XylNC (Xyl = 2,6-$Me_2C_6H_3$) and **2a** in C_6H_5Cl to form the cationic iminoacyl complex [(BDI)(η^2-XylN═CMe)Nb(N^{t}Bu)][B(C_6F_5)$_4$] (**9**, Scheme 7). The reaction mixture immediately turned dark red on addition of the isocyanide, then golden yellow within seconds. A ^{1}H NMR spectrum of the reaction mixture revealed the presence of two products, as indicated by the appearance of two new BDI methine resonances at 5.84 and 5.83 ppm. We attribute these signals to the stereoisomers generated by the variable orientation of the η^2-iminoacyl ligand (Scheme 7). A VT NMR experiment confirmed this assignment: on heating the sample to 343 K the resonances for the BDI backbone methine coalesced into a single signal. The remainder of the spectrum was broad and largely unidentifiable at this temperature (and up to 398 K), but cooling the sample back to room temperature caused the two original

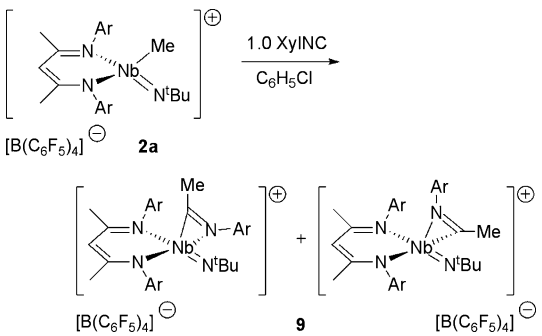

Scheme 7

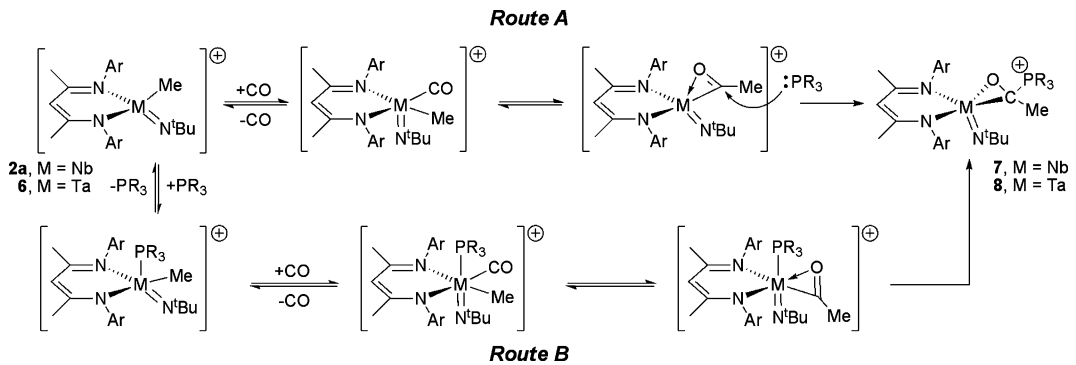

Scheme 6 Possible mechanisms leading from compound **2a**(**6**) to compound **7**(**8**).

 This journal is © The Royal Society of Chemistry 2011

Published on 27 April 2011. Downloaded by University of Chicago on 30/10/2014 19:42:54.

resonances to reappear, as the isomers resolved relative to the NMR timescale. An IR spectrum of **9** further supported the proposed formulation. Due to the reduced N–C bond order within the iminoacyl group, the N–C stretching frequency in the IR spectrum shifts to lower frequencies. A stretch attributable to **9** was observed at 1642 cm^{-1}.

As further confirmation of the proposed structure of **9**, addition of 1.0 equiv of MeMgBr in Et_2O resulted in a rapid reaction to give the η^2-ketimine complex (BDI)(η^2-XylN=CMe_2)Nb(N^{t}Bu) (**10**) in near quantitative yield. Complex **10** was described previously as the product resulting from the reaction of **1** with 1.0 equiv of XylNC,[53] and the synthesis of **10** from **9** supports the intermediacy of the iminoacyl complex during the formation of **10** from **1** directly. This reaction parallels the addition of nucleophiles to organic imines and ketones, whereby the transition metal can be considered to act as both a Lewis acid binding to the N/O group and as an electron-withdrawing carbon-bound leaving group, activating the unsaturated carbon toward nucleophilic attack. In the present system, the methyl group could add either to the iminoacyl carbon or to the formally cationic metal center. In the latter case, subsequent methyl group transfer to the iminoacyl carbon would then furnish **10** (Scheme 8). This latter process would mimic the assumed mechanism for the formation of the ketimine complex from the reaction of **1** with XylNC, but the electrophilic character of the iminoacyl may be sufficient to promote attack by the incoming nucleophile directly. The direct addition mechanism would be related to the attack of a nucleophile on an organic imine or iminium carbon.

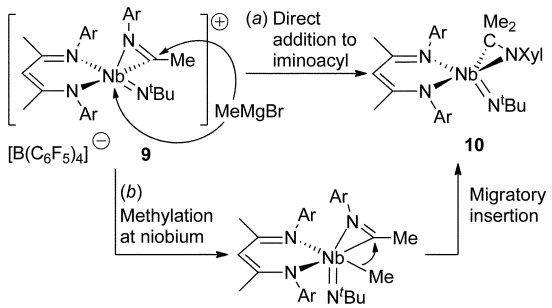

Scheme 8

Since the acyl and iminoacyl complexes are isolobal, we were interested to see if the iminoacyl cations would coordinate phosphines in a manner analogous to that observed for the acyl compounds described above; however, no reaction was observed between **9** and PEt_3 at room temperature. This lack of reactivity between the phosphine and the iminoacyl carbon compared to the facile formation of the phosphine-trapped acyls is supported by theoretical studies that have predicted a higher energy π^*_{CN} orbital on iminoacyl ligands compared to that of the corresponding π^*_{CO} orbital of an acyl,[67] but the lack of reactivity may also reflect the different steric properties imposed by the bulky 2,6-xylyl substituent on the iminoacyl nitrogen.

Related insertion reactions with 2a and 6

In contrast to the behavior of **1**, the cation **2a** underwent 1,2-insertion reactions with several unsaturated organic substrates at room temperature, but no reaction was observed between **2a** and terminal or internal aryl alkynes, PhNCO, ^{t}BuNCS, or propylene oxide. The stability of this complex toward such reagents under these conditions (low-polarity solvents, 20 °C, 1 atm pressure) is reminiscent of a structurally related imidotitanium BDI complex.[68]

Addition of stoichiometric amounts of acetophenone to solutions of **2a** or **6** in fluorobenzene cleanly led to the alkoxide complexes [(BDI)(PhMe$_2$CO)M(N^{t}Bu)][B(C$_6$F$_5$)$_4$] (**11**, M = Nb; **12** M = Ta; Scheme 9) by insertion of acetophenone into the M–Me bond. The ^{1}H NMR spectra of the products indicate average C_s-symmetry. A new, sharp singlet appears in the range of 1.60–1.70 ppm for each compound, which integrates to 6H relative to one equivalent of the BDI ligand. Assignment of this signal to the equivalent methyl groups on the alkoxide ligand was supported by an HMBC ^{1}H-^{13}C correlation experiment that revealed this signal to be within three bonds of a carbon with a chemical shift between 85 and 90 ppm. Only one ^{13}C{^{1}H} NMR resonance was observed above 170 ppm for each compound, and those signals are attributable to the two symmetry-related imine carbons of the BDI ligand. Similarly, no IR stretches were observed in the ketone region of the spectra of the isolated products.

On addition of the carbodiimide CyN=C=NCy to a solution of **2a** in chlorobenzene, the solution turned from yellow to bright

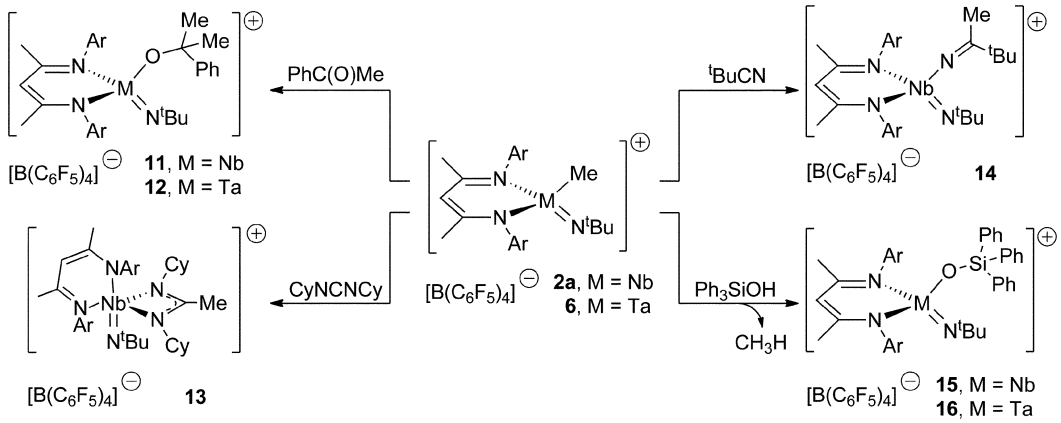

Scheme 9

Published on 27 April 2011. Downloaded by University of Chicago on 30/10/2014 19:42:54.

red over the course of 3 h, affording the κ^2-amidinate complex [(BDI){κ^2-N_2-MeC(NCy)$_2$}Nb(N^{t}Bu)][B(C$_6$F$_5$)$_4$] (**13**, Scheme 9). Complex **13** has averaged C_s symmetry in solution by ^{1}H NMR spectroscopy as judged by the appearance of a single pentet integrating to 2H at 2.66 ppm that corresponds to the two N-C*H*(c-C$_5$H$_{10}$) protons. A new singlet at 1.84 ppm is assigned to the amidinate methyl group (*Me*CN$_2$), and the ^{13}C{^{1}H} NMR spectrum has both a new amidinate carbon resonance at 185.5 ppm (N*C*N) and a new amidinate methyl resonance at 13.9 ppm (NC(*Me*)N), which is shifted considerably upfield from that observed for the cation. The IR spectrum of **13** shows a signal at 1643 cm^{-1} due to the amidinate NCN functionality, consistent with analogous bands in other early transition metal complexes.[69]

A related insertion process occurred upon the reaction of **2a** with ^{t}BuCN to form the cationic Nb ketimide [(BDI)(^{t}BuMeC═N)Nb(N^{t}Bu)][B(C$_6$F$_5$)$_4$] (**14**; Scheme 9). The ^{1}H NMR signal for the Nb–Me group shifts from 0.95 ppm for **2a** to 1.31 ppm for **14**.[70] Notably, the ^{1}H NMR spectrum for **14** displays broad signals, indicating that interconversion of the two possible ketimide regioisomers is occurring at room temperature at a rate close to the NMR timescale. A variable temperature NMR study in C$_6$H$_5$Cl reveals that the broadened signals sharpen upon heating to 343 K, indicating the presence of a single complex with overall C_s symmetry. On cooling to 223 K, the single broad resonance observed at 5.55 ppm at room temperature for the BDI methine proton decoalesces into two non-equivalent singlets in a 2.5 : 1 ratio, with resonances at 5.29 and 5.58 ppm, respectively.

Reaction of cations 2a and 6 with Ph$_3$SiOH

The stability of the cationic complexes toward a protic silanol reagent was also investigated. On addition of a solution of 1.0 equiv of Ph$_3$SiOH in fluorobenzene to a solution of either **2a** or **6** in fluorobenzene the solution rapidly effervesced, yielding [(BDI)(Ph$_3$SiO)M(N^{t}Bu)][B(C$_6$F$_5$)$_4$] (**15**, M = Nb; **16**, M = Ta; Scheme 9) in quantitative yields as the product resulting from clean protonolysis of the M–Me group. By comparison, the methyl-bound cationic complexes were stable in the presence of an excess of [(Et$_2$O)$_2$H][B(C$_6$F$_5$)$_4$] at room temperature, indicating that a coordinating counter-ion is needed to effect methane loss. Similarly, the methyl-bound cations were found to be stable toward reaction with H$_2$ at elevated temperatures (75 °C for **2a** and 135 °C for **6**). The siloxide complexes are thermally robust, persisting in solution at 135 °C for days without decomposition.

Polymerization of ethylene with 2b

Since early-transition metal imido-supported alkyl cations are well-known to effect olefin polymerization,[3,21–23] we tested our systems for this capability. The Ta cation **6** failed to give appreciable quantities of polyethylene, but exposure of a solution of **2b** (0.5 mol%, 0.002 M) in C$_6$H$_5$Cl to 200 equiv of ethylene (1 atm) at room temperature caused a white solid to precipitate after stirring for 12 h. The solid that formed was collected (>90%, see experimental section) and identified as high-density polyethylene, having a sharp melting point at 122 °C. Other α-olefins (both branched and linear) failed to yield polymer in appreciable quantities under these conditions.

Summary and conclusions

The neutral dimethyl complexes **1** (Nb) and **5** (Ta) undergo clean methide group protonolysis to yield the stable 12/14 e$^-$ cations **2a** and **6**. These compounds have been thoroughly characterized and, for **2a**, confirmed structurally. The crystallographic data indicate a shortening of the Nb–Me and Nb═N^{t}Bu bonds relative to those observed for **1**, which is indicative of a complex with both a lower coordination number and higher metal-based cationic charge.

In contrast to the divergent carbonylation chemistry observed with the dimethyl compounds, the methyl cations were not found to irreversibly bind CO. In the presence of phosphines, cationic phosphine-trapped acyl species could be formed cleanly as either a single (PCy$_3$) or a mixture (PEt$_3$) of isomers. When isotopically enriched ^{13}CO was used in the reaction, these complexes were readily identified by diagnostic doublets ($^1J_{CP} \approx 50$ Hz) in the ^{13}C{^{1}H} and ^{31}P{^{1}H} NMR. The coupling constants and the associated chemical shift ranges of the doublets coincide well with those of analogous complexes.

A related insertion reaction with XylNC was observed to yield a stable cationic iminoacyl species as a mixture of two isomers. This compound was stable in solution up to 398 K and, in contrast to the acyls, did not bind phosphines to yield tetrahedral phosphine-trapped iminoacyls. The relative stability of these compounds, and related iminoacyl complexes as a whole, compared to that of their isoelectronic acyl counterparts has been documented in the literature.[54]

The cationic complexes **2a** and **6** underwent insertion reactions with acetophenone to yield cationic alkoxide complexes, and **2a** inserted CyN═C═NCy and ^{t}BuCN to yield the amidinate and ketimide complexes, respectively. Both the Ta and Nb complexes cleanly extruded methane on reaction with Ph$_3$SiOH to yield the siloxide complexes in high yields.

Finally, while the Ta cation was not observed to polymerize ethylene, the Nb complex **2b** afforded high-density polyethylene in high yield at room temperature under 1 atm of pressure. The niobium cation failed to yield appreciable quantities of poly(α-olefins) when polymerization reactions were screened under similar conditions with both branched and linear α-olefins, indicating that the steric requirements of the BDI ligand allow only the smallest substrates to enter the coordination sphere of the metal.

Taken together, these data indicate that the Nb/Ta imido linkages for these complexes, when in the presence of a Nb/Ta alkyl bond, do not react irreversibly with a range of unsaturated organic molecules. Furthermore, complexes **2a, b** and **6** are isoelectronic analogues to similarly unreactive and structurally analogous Ti complexes,[68] suggesting that the early-metal (BDI)M(NR) framework may provide a general, robust platform for the investigation of non-metallocene, early-metal alkyl chemistry.

Notes and references

1 P. D. Bolton, E. Clot, N. Adams, S. Dubberley, A. Cowley and P. Mountford, *Organometallics*, 2006, **25**, 2806–2825.
2 L. L. Anderson, J. A. R. Schmidt, J. Arnold and R. Bergman, *Organometallics*, 2006, **25**, 3394–3406.
3 N. Adams, H. J. Arts, P. D. Bolton, D. Cowell, S. R. Dubberley, N. Friederichs, C. Grant, M. Kranenburg, A. J. Sealey, B. Wang, P. J. Wilson, A. R. Cowley, P. Mountford and M. Schröder, *Chem. Commun.*, 2004, 434.

 This journal is © The Royal Society of Chemistry 2011

Published on 27 April 2011. Downloaded by University of Chicago on 30/10/2014 19:42:54.

4 A. Martin, R. Uhrhammer, T. G. Gardner, R. F. Jordan and R. D. Rogers, *Organometallics*, 1998, **17**, 382–397.
5 T. Tsukahara, D. C. Swenson and R. F. Jordan, *Organometallics*, 1997, **16**, 3303–3313.
6 E. B. Tjaden, D. C. Swenson, R. F. Jordan and J. L. Petersen, *Organometallics*, 1995, **14**, 371–386.
7 A. Guram, R. Jordan and D. Taylor, *J. Am. Chem. Soc.*, 1991, **113**, 1833–1835.
8 M. Bochmann, *J. Chem. Soc., Dalton Trans.*, 1996, 255–270.
9 H. H. Brintzinger, D. Fischer, R. Mülhaupt, B. Rieger and R. M. Waymouth, *Angew. Chem., Int. Ed. Engl.*, 1995, **34**, 1143–1170.
10 T. J. Marks, *Acc. Chem. Res.*, 1992, **25**, 57–65.
11 R. F. Jordan, *Adv. Organomet. Chem.*, 1991, **32**, 325–387.
12 D. W. Stephan, *Organometallics*, 2005, **24**, 2548–2560.
13 M. Mitani, J. Saito, S. Ishii, Y. Nakayama, H. Makio, N. Matsukawa, S. Matsui, J. Mohri, R. Furuyama, H. Terao, H. Bando, H. Tanaka and T. Fujita, *Chem. Rec.*, 2004, **4**, 137–158.
14 V. C. Gibson and S. K. Spitzmesser, *Chem. Rev.*, 2003, **103**, 283–315.
15 L. Resconi, L. Cavallo, A. Fait and F. Piemontesi, *Chem. Rev.*, 2000, **100**, 1253–1345.
16 S. D. Ittel, L. K. Johnson and M. Brookhart, *Chem. Rev.*, 2000, **100**, 1169–1203.
17 W. Kaminsky, *J. Chem. Soc., Dalton Trans.*, 1998, 1413–1418.
18 X. Bei, D. C. Swenson and R. F. Jordan, *Organometallics*, 1997, **16**, 3282–3302.
19 I. Kim, Y. Nishihara, R. F. Jordan, R. D. Rogers, A. L. Rheingold and G. P. A. Yap, *Organometallics*, 1997, **16**, 3314–3323.
20 H. H. Brintzinger, D. Fischer, R. Mülhaupt, B. Rieger and R. M. Waymouth, *Angew. Chem., Int. Ed. Engl.*, 1995, **34**, 1143–1170.
21 P. D. Bolton and P. Mountford, *Adv. Synth. Catal.*, 2005, **347**, 355–366.
22 G. J. Hayday, C. Wang, N. H. Rees and P. Mountford, *Dalton Trans.*, 2008, 3301.
23 H. Bigmore, S. Dubberley, M. Kranenburg, S. Lawrence, A. Sealey, J. Selby, M. Zuideveld, A. Cowley and P. Mountford, *Chem. Commun.*, 2006, 436.
24 A. P. Duncan and R. G. Bergman, *Chem. Rec.*, 2002, **2**, 431–445.
25 W. A. Nugent and J. M. Mayer, *Metal–Ligand Multiple Bonds*, John Wiley & Sons, New York, 1988.
26 R. E. Blake, Jr., D. M. Antonelli, L. M. Henling, W. P. Schaefer, K. I. Hardcastle and J. E. Bercaw, *Organometallics*, 1998, **17**, 718–725.
27 C. P. Schaller, C. C. Cummins and P. T. Wolczanski, *J. Am. Chem. Soc.*, 1996, **118**, 591–611.
28 D. Wigley, *Prog. Inorg. Chem.*, 1994, **42**, 239–482.
29 C. P. Schaller and P. T. Wolczanski, *Inorg. Chem.*, 1993, **32**, 131–144.
30 J. de With and A. D. Horton, *Angew. Chem., Int. Ed. Engl.*, 1993, **32**, 903–905.
31 J. de With, A. D. Horton and A. G. Orpen, *Organometallics*, 1993, **12**, 1493–1496.
32 C. C. Cummins, C. P. Schaller, G. D. Van Duyne, P. T. Wolczanski, A. W. E. Chan and R. Hoffmann, *J. Am. Chem. Soc.*, 1991, **113**, 2985–2994.
33 P. D. Bolton, M. Feliz, A. Cowley, E. Clot and P. Mountford, *Organometallics*, 2008, **27**, 6096–6110.
34 B. D. Ward, G. Orde, E. Clot, A. R. Cowley, L. H. Gade and P. Mountford, *Organometallics*, 2005, **24**, 2368–2385.
35 P. D. Bolton, E. Clot, A. Cowley and P. Mountford, *Chem. Commun.*, 2005, 3313.
36 B. D. Ward, G. Orde, E. Clot, A. R. Cowley, L. H. Gade and P. Mountford, *Organometallics*, 2004, **23**, 4444–4461.
37 P. Legzdins, E. C. Phillips, S. J. Rettig, J. Trotter, J. E. Veltheer and V. C. Yee, *Organometallics*, 1992, **11**, 3104–3110.
38 P. J. Alaimo, D. W. Peters, J. Arnold and R. G. Bergman, *J. Chem. Educ.*, 2001, **78**, 64–64.
39 P. H. M. Budzelaar, A. B. van Oort and A. G. Orpen, *Eur. J. Inorg. Chem.*, 1998, 1485–1494.
40 S. Schmidt and J. Sundermeyer, *J. Organomet. Chem.*, 1994, **472**, 127–138.
41 P. Jutzi, C. Müller, A. Stammler and H. G. Stammler, *Organometallics*, 2000, **19**, 1442–1444.
42 N. C. Tomson, J. Arnold and R. G. Bergman, *Organometallics*, 2010, **29**, 2926–2942.
43 *SMART: Area-Detector Software Package,* Bruker Analytical X-ray Systems, Inc., Madison, WI, 2001–2003.
44 *SAINT: SAX Area-Detector Integration Program*, V6.40; Bruker Analytical X-ray Systems Inc., Madison, WI, 2003.
45 *XPREP*; Bruker Analytical X-ray Systems Inc., Madison, WI, 2003.
46 *SADABS: Bruker-Nonius Area Detector Scaling and Absorption v. 2.05,* Bruker Analytical X-ray Systems, Inc., Madison, WI, 2003.
47 L. J. Farrugia, *J. Appl. Crystallogr.*, 1997, **30**, 565.
48 Z. Lin and M. B. Hall, *Coord. Chem. Rev.*, 1993, **123**, 149–167.
49 J. T. Ciszewski, J. F. Harrison and A. L. Odom, *Inorg. Chem.*, 2004, **43**, 3605.
50 M. Humphries, M. Green, M. Leech, V. Gibson, M. Jolly, D. Williams, M. Elsegood and W. Clegg, *J. Chem. Soc., Dalton Trans.*, 2000, 4044–4051.
51 A. D. Horton, J. de With, A. J. van der Linden and H. van de Weg, *Organometallics*, 1996, **15**, 2672–2674.
52 Determined using the continuous symmetry parameter $\tau = (\alpha - \beta)/60$, where α and β are the largest and second largest angles about the metal center, respectively: A. W. Addison, T. N. Rao, J. Reedijk, J. van Rijn and G. C. Verschoor, *J. Chem. Soc., Dalton Trans.*, 1984, 1349.
53 N. C. Tomson, A. Yan, J. Arnold and R. G. Bergman, *J. Am. Chem. Soc.*, 2008, **130**, 11262–11263.
54 L. Durfee and I. Rothwell, *Chem. Rev.*, 1988, **88**, 1059–1079.
55 J. A. Marsella, K. Moloy and K. G. Caulton, *J. Organomet. Chem.*, 1980, **201**, 389–398.
56 M. D. Fryzuk, M. Mylvaganam, M. Zaworotko and L. MacGillivray, *Organometallics*, 1996, **15**, 1134–1138.
57 W. Tikkanen, A. Kim, K. Lam and K. Ruekert, *Organometallics*, 1995, **14**, 1525–1528.
58 A. Martín, M. Mena, M. A. Pellinghelli, P. Royo, R. Serrano and A. Tiripicchio, *J. Chem. Soc., Dalton Trans.*, 1993, 2117–2122.
59 W. Tikkanen and J. Ziller, *Organometallics*, 1991, **10**, 2266–2273.
60 J. Arnold, T. D. Tilley, A. L. Rheingold, S. J. Geib and A. M. Arif, *J. Am. Chem. Soc.*, 1989, **111**, 149–164.
61 P. V. Bonnesen, P. K. L. Yau and W. H. Hersh, *Organometallics*, 1987, **6**, 1587–1590.
62 J. Arnold, T. D. Tilley and A. L. Rheingold, *J. Am. Chem. Soc.*, 1986, **108**, 5355–5356.
63 H. H. Karsch, G. Müller and C. Krüger, *J. Organomet. Chem.*, 1984, **273**, 195–212.
64 J. A. Labinger, J. N. Bonfiglio, D. L. Grimmett, S. T. Masuo, E. Shearin and J. S. Miller, *Organometallics*, 1983, **2**, 733–740.
65 D. L. Grimmett, J. A. Labinger, J. N. Bonfiglio, S. T. Masuo, E. Shearin and J. S. Miller, *Organometallics*, 1983, **2**, 1325–1332.
66 J. A. Labinger and J. S. Miller, *J. Am. Chem. Soc.*, 1982, **104**, 6856–6858.
67 L. Durfee, A. McMullen and I. Rothwell, *J. Am. Chem. Soc.*, 1988, **110**, 1463–1467.
68 F. Basuli, J. C. Huffman and D. J. Mindiola, *Inorg. Chem.*, 2003, **42**, 8003–8010.
69 A. E. Guiducci, C. L. Boyd and P. Mountford, *Organometallics*, 2006, **25**, 1167–1187.
70 D. R. Armstrong, K. W. Henderson, I. Little, C. Jenny, A. R. Kennedy, A. E. McKeown and R. E. Mulvey, *Organometallics*, 2000, **19**, 4369–4375.